Cancer Science
Japanese Cancer Association JCA
Open Access

Anti-PD-L1 treatment enhances antitumor effect of everolimus in a mouse model of renal cell carcinoma

Yukiyoshi Hirayama,[1,2] Min Gi,[1] Shotaro Yamano,[1] Hirokazu Tachibana,[2] Takahiro Okuno,[1] Satoshi Tamada,[2] Tatsuya Nakatani[2] and Hideki Wanibuchi[1]

Departments of [1]Molecular Pathology; [2]Urology, Osaka City University Graduate School of Medicine, Osaka, Japan

Key words

Everolimus, immune checkpoint, PD-1, PD-L1, renal cell carcinoma

Correspondence

Hideki Wanibuchi, Department of Molecular Pathology, Osaka City University Graduate School of Medicine, 1-4-3 Asahi-machi, Abeno-ku, Osaka 545-8585, Japan.
Tel: +81-6-6645-3737; Fax: +81-6-6-6646-3093;
E-mail: wani@med.osaka-cu.ac.jp

Funding Information

Japan Society for the Promotion of Science (16K20157); Smoking Research Foundation.

Received July 16, 2016; Revised October 1, 2016; Accepted October 4, 2016

Cancer Sci **107** (2016) 1736–1744

doi: 10.1111/cas.13099

Immunotherapy based on blockade of the programmed death-1 (PD-1)/programmed death-ligand 1 (PD-L1) axis has shown promising clinical activity for renal cell carcinoma (RCC) patients; however, the most effective use of these agents in combination with conventional targeted therapy remains to be resolved. Here we evaluated the therapeutic efficacy of the combination of the mTOR inhibitor everolimus (EVE) and anti-PD-L1 using an immunocompetent mouse model of RCC. We first assessed the *in vitro* effect of EVE on PD-L1 expression in the human 786-O and mouse RENCA RCC cell lines and found that EVE upregulated PD-L1 expression in these RCC cell lines. We then treated RENCA tumor-bearing mice with EVE and found that PD-L1 expression was also increased in tumor cells after EVE treatment. To determine the antitumor effects of EVE alone, anti-PD-L1 alone, and EVE in combination with anti-PD-L1, we evaluated their antitumor effects on RENCA tumor-bearing mice. A significant decrease in the tumor burden was observed in the EVE alone but not in the anti-PD-L1 alone treatment group compared with the control group. Importantly, the combination of EVE with anti-PD-L1 significantly reduced tumor burden compared with the EVE alone treatment, increasing tumor infiltrating lymphocytes (TILs) and the ratio of cytotoxic CD8$^+$ T cells to TILs. The results of the present study demonstrated that anti-PD-L1 treatment enhanced the antitumor effect of EVE in a mouse model, supporting a direct translation of this combination strategy to the clinic for the treatment of RCC.

Each year, approximately 338 000 patients are newly diagnosed with kidney cancer worldwide.[1] Renal cell carcinoma (RCC) constitutes 85% of kidney cancers and accounts for 3% of adult malignancies.[2] Overall, several targeted drugs have been approved since 2005 for the treatment of advanced RCC and include vascular endothelial growth factor (VEGF) pathway inhibitors and mammalian target of rapamycin (mTOR) inhibitors.[3] Everolimus (EVE) is an mTOR inhibitor that is recommended for patients with metastatic RCC after the failure of anti-VEGF therapy.[4,5] However, despite the development of targeted therapies, most patients develop resistance following an initial response to therapy and eventually die of their disease. Therefore, novel therapeutic approaches are urgently needed to improve the outcomes of RCC patients.

Since RCC is considered an immunogenic tumor, several immunotherapies have been attempted in the past.[6] Currently, immune checkpoint inhibitors have shown considerable potential in the treatment of multiple types of malignancies including RCC.[7–9] Programmed death-ligand 1 (PD-L1) is a key immune checkpoint molecule belonging to the B7 family and can facilitate immune evasion and T cell exhaustion.[10] PD-L1 is expressed in wide variety of solid tumors and negatively regulates T-cell signaling through binding to its receptor, programmed death-1 (PD-1), on tumor-specific T cells. As a result, increased PD-L1 expression by cancer cells is a fundamental host immune escape mechanism.[11,12] The importance of the immune checkpoint PD-1/PD-L1 in RCC is reflected by the antitumor activities of anti-PD-1/L1 antibody in previously treated RCC patients.[13,14]

However, many issues remain to be resolved: clinicians are now faced with questions about the optimal combination of the current treatments with anti-PD-1/PD-L1 antibodies. Recently the combination of anti-angiogenic therapy with immunotherapy based on the blockade of the PD-1/PD-L1 axis has been evaluated in clinical trials to assess the safety, tolerability, and benefit in advanced RCC patients (NCT02231749, NCT01633970).[6] Currently, there are no studies that are examining the combination of an mTOR inhibitor with anti-PD-1/PD-L1 on RCC patients.

Although PD-L1 has been reported to be overexpressed in several human malignancies and links to poor prognosis and resistance to anticancer therapies in RCC,[15–17] the precise mechanism of PD-L1 expression remains unclear. It has been shown that interferons and cytokines are potent upregulators of PD-L1 expression.[7,18] In addition, anticancer therapy such as chemotherapy and radiotherapy can induce PD-

L1 expression in bladder cancer and RCC.[19,20] However, the effects of mTOR inhibition on the tumor immune microenvironment and PD-L1 expression in RCC are unclear. Thus, the effect of an mTOR inhibitor on tumor PD-L1 expression and PD-1/PD-L1 blockade should be evaluated to determine if an mTOR inhibitor can be used in combination with immune checkpoint inhibition for RCC treatment.

Herein we evaluated the therapeutic efficacy of the combination of the mTOR inhibitor EVE and anti-PD-L1 using an immunocompetent mouse model. We also evaluated the correlation between PD-L1 expression and EVE treatment that might provide new insights into the development of immune-based therapy in RCCs.

Materials and Methods

Cell lines and reagents. The human RCC cell line 786-O and mouse RCC cell line RENCA were obtained from American Type Culture Collection (Rockville, MD, USA). Both cell lines were cultured in RPMI 1640 supplemented with 10% fetal bovine serum, 100 IU/mL penicillin, and 100 μg/mL streptomycin. They were grown in a humidified incubator with 5% CO_2 at 37°C. EVE and MK2206 were purchased from Selleck (San Diego, CA, USA). Rapamycin and LY294002 were purchased from Calbiochem (LaJolla, CA, USA). Anti-mouse PD-L1 (clone 10F.9G2) and IgG isotype control (clone LTF-2) were purchased from Bio-XCell (West Lebanon, NH, USA).

Flow cytometry. To assess cell surface PD-L1 expression, cells were harvested and stained with PE-conjugated anti-mouse PD-L1 antibody or mouse IgG isotype control antibody (eBiosceience, San Diego, CA, USA). After incubation for 30 min at 4°C, cells were washed with FCM buffer and the mean fluorescence intensity (MFI) of PD-L1 was analyzed using a MoFlo XDP and Summit software (Beckman Coulter, Brea, CA, USA). To obtain single-cell suspensions from xenografted tumors, tumor tissues were digested with 1 mg/mL collagenase/dispase (Sigma-Aldrich, St Louis, MO, USA) for 45 min at 37°C and red blood cells were removed using PharmLyse (BD Biosciences, Franklin Lakes, NJ, USA). Cells were co-stained with APC-conjugated anti-mouse CD45 antibody (Miltenyli Biotech, Bergisch Gladbach, Germany) and PE-conjugated anti-mouse-PD-L1 antibody and analyzed for the $CD45^-$ cell fraction.

Quantitative real time-PCR. RNA was extracted with Trizol (Invitrogen, Carlsbad, CA, USA) according to the manufacturer's protocol. Reverse transcription reactions were conducted using Advantage RT-for-PCR kit (Takara Bio, Tokyo, Japan). The cDNA was amplified using TaqMan Universal PCR Master Mix (Applied Biosystems, Foster City, CA, USA) with the Applied Biosystems 7500 Fast real-time PCR machine (Applied Biosystems) and predeveloped TaqMan assay primers and probes (human CD274, Hs00234244_m1; mouse CD274, Mm00452054_m1; all from Applied Biosystems). Data were normalized to 18s gene expression.

Western blot analysis. Protein was extracted with lysis buffer, a mixture of RIPA buffer [Cell Signaling Technology (CST), Danvers, MA, USA] and protease inhibitor cocktails (Sigma-Aldrich). The amount of protein was determined using a BCA protein assay kit (Pierce, Rockford, IL, USA). Equal amounts of denatured proteins were separated by electrophoresis on sodium dodecyl sulfate–polyacrylamide gel electrophoresis (SDS–PAGE) gels and transferred to a polyvinylidene fluoride (PVDF) membrane and blocked with 2% bovine serum albumin (BSA) in tris buffered saline (TBS) containing 0.1% Tween-20. The membranes were probed with the following primary antibodies: anti-S6 (#2708) diluted 1:1000, anti-phosoho-S6 (#4858) diluted 1:1000, anti-AKT (#9272) diluted 1:1000, anti-phospho-AKT (#4056) (CST) diluted 1:1000, and anti-β-actin (Merck Millipore, Billerica, MA, USA) diluted 1:1000, and subsequently incubated with horse radish peroxidase (HRP)-conjugated secondary antibody (Santa Cruz Biotechnology, Dallas, TX, USA). To detect reactive bands, the membranes were examined using the ECL Prime Western Blotting Detection System (GE Healthcare, Amersham, UK) and LAS-3000 (Fujifilm, Tokyo, Japan).

Proliferation assay. Cells were seeded onto 96-well plates (RENCA 10 000 cells per well, 786-O 2500 cells per well) and allowed to attach overnight. After 48 h of vehicle or drug treatment, cell proliferation assays were performed using Cell Counting Kit-8 (DOJINDO, Tokyo, Japan) according to the manufacturer's instructions. Absorbance was measured with a microplate reader (Bio-Rad, Tokyo, Japan) at 450 nm.

Animal studies. The animal experiment protocols were approved by The Laboratory Animal Center of Osaka City University Graduate School of Medicine, which is accredited by the Center for the Accreditation of Laboratory Animal Care and Use (CALAC), Japan Health Sciences Foundation (JHSF). Eight week-old-male Balb/c mice were purchased from Japan SLC (Shizuoka, Japan). RENCA cells (5×10^6) were suspended in 50 μL phosphate-buffered saline (PBS) and an equal volume of Matrigel Growth Factor Reduced (Corning, NY, USA) and subcutaneously injected into the backs of mice. EVE was prepared in 30% propylene glycol and 5% Tween 80 (vehicle). In the study to examine PD-L1 expression induced by EVE, mice were treated with vehicle or EVE (0.25 mg/kg EVE, every day, p.o.) when the tumors reached approximately 100 mm^3 in volume. The dose of EVE was selected based on the results of our preliminary study in which 0.25 mg/kg EVE significantly inhibited RENCA xenograft growth. After 7 days of treatment, the mice were killed and the tumors were processed for immunohistochemical (IHC) staining and flow cytometry (FCM) analysis. In the co-administration study, mice were divided into four groups and treated when the tumors reached approximately 100 mm^3 in volume as follows: Control group (vehicle and isotype IgG control), EVE group (0.25 mg/kg EVE, five times a week, p.o.), anti-PD-L1 group (200 μg anti-PD-L1/mouse, twice a week, i.p.), and combination treatment group (concurrent treatment with EVE and anti-PD-L1). Body weight and tumor volume were measured twice a week. The tumor volume was calculated using the empirical formula $V = 1/2 \times [(\text{shortest diameter})^2 \times (\text{the longest diameter})]$. After 2 weeks of treatment, the mice were killed and the tumors were weighed and processed for IHC analysis.

Immunohistochemical studies. Immunohistochemistry was performed in formalin fixed paraffin embedded (FFPE) sections and OCT-embedded frozen tissue sections. FFPE RENCA tumor sections were cut (3 μm) and deparaffinized in xylene and rehydrated in a graded series of alcohol and distilled water. Endogenous peroxidase was blocked with 3% hydrogen peroxide in distilled water for 5 min. Non-specific binding was blocked with normal horse serum at 37°C for 30 min. Sections were then incubated with pS6 (#4858, CST) diluted 1:500, p4EBP-1 (#2855, CST) diluted 1:1000, Granzyme B (ab4059, Abcam, Cambridge, MA, USA) diluted in 1:100, Foxp3 diluted in 1:500 (ab20034, Abcam), or Ki67 (ab16667, Abcam) diluted 1:500. Detection was completed using the VETASTAIN ABC Kit (Vector Laboratories, Burlingame, CA, USA) according to the manufacturer's instructions. Frozen sections were cut

(5 μm) and fixed by formalin for 2 min. The sections were blocked with normal horse serum and incubated with primary antibody as follows: anti-PD-L1 (eBioscience, San Diego, CA, USA) diluted 1:500, cleaved caspase 3 (#9664, CST) diluted in 1:1000, anti-CD3 (Abcam) diluted 1:500, or biotinized anti-CD8 (eBioscience) diluted 1:200. Immunoreactivity was detected by Alexafluor-488, Alexafluor-594, or Alexafluor-594 streptavidin conjugated second antibodies (Invitrogen). Nuclei were counterstained with DAPI (Vector Laboratories). For TUNEL staining, the ApopTag Fluorescein In Situ Apoptosis Detection Kit (Millipore, Billerica, MA, USA) was used according to the manufacturer's instructions. All images were captured using BZ-X700 (KEYENCE, Osaka, Japan). Ki67, TUNEL, Granzyme B, Foxp3, CD3, and CD8 stains were quantified by counting the number of positive cells.

Statistics. Statistical analysis was carried out with GraphPad Prism version 5.0 software (GraphPad Software, San Diego, CA, USA). Data are represented as the mean ± SEM for all figure panels in which error bars are shown. Homogeneity of variance was tested by the *F*-test. The *P*-values were assessed using two-tailed Student *t*-tests when the variance was homogeneous and two-tailed Welch's *t*-tests when the variance was heterogeneous. *P*-values < 0.05 were considered statistically significant.

Results

EVE induces PD-L1 surface expression *in vitro*. We first assessed the effect of EVE on PD-L1 surface expression by flow cytometry and on PD-L1 mRNA level by quantitative real-time PCR in the human RCC cell line 786-O and the mouse RCC cell line RENCA. RCC cells were treated with different concentrations of EVE (0, 0.1, 1, 10 100 nM) for 72 h. We found that the surface expression of PD-L1 was upregulated in both 786-O and RENCA cells in a dose dependent manner (Fig. 1a,b). We next treated RCC cells with

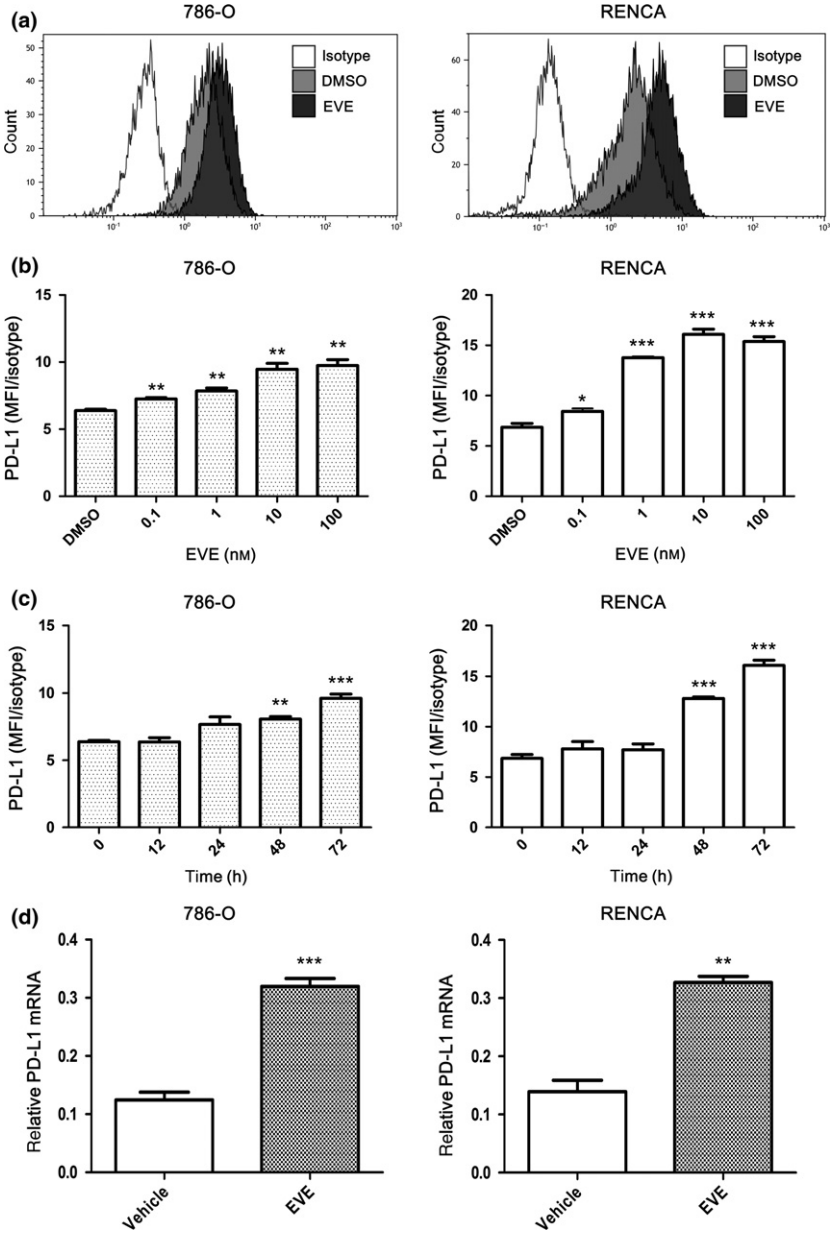

Fig. 1. Everolimus (EVE) induces programmed death-ligand 1 (PD-L1) expression in renal cell carcinoma cell lines 786-O and RENCA. (a) Representative histogram of PD-L1 expression in 786-O and RENCA cells. (b) After 786-O and RENCA cells were treated with EVE (0, 0.1, 1.0, 10, 100 nM) for 72 h, PD-L1 expression was analyzed by flow cytometry (FCM). MFI, mean fluorescence intensity. (c) After 786-O and RENCA cells were treated with EVE (10 nM) for 0–72 h, PD-L1 expression was analyzed by FCM. (d) PD-L1 mRNA in 786-O and RENCA cells treated with EVE (10 nM) for 72 h was measured and normalized to 18s. **P* < 0.05; ***P* < 0.01; ****P* < 0.001.

10 nM EVE for different times (0, 12, 24, 48, 72 h). We observed a time-dependent increase in surface PD-L1 expression in both 786-O and RENCA cells (Fig. 1c). This was consistent with the results of PD-L1 mRNA levels (Fig. 1d). These results suggest that EVE upregulates PD-L1 expression in RCC cell lines in a time- and dose-dependent manner. In order to verify whether PD-L1 expression is correlated with active AKT-PI3K-mTOR signaling, we treated RCC cells with inhibitors of PI3K (ly294002), AKT (mk2206), or mTOR (rapamycin). Interestingly, PD-L1 expression in 786-O and RENCA cells was upregulated by rapamycin in a dose- and time-dependent manner, but not by mk2206 or ly294002 (Fig. S1). Therefore, PD-L1 expression was specifically elevated by an mTOR inhibitor. These results suggest the existence of upregulators of PD-L1 in genes responding to the inhibition of mTOR, but not in those responding to the inhibition of PI3K or AKT in 786-O and RENCA cells.

***In vitro* EVE but not anti-PD-L1 inhibits tumor cell proliferation.** To investigate the effect on RCC cell proliferation *in vitro*, we treated RENCA cells with different concentrations of EVE (0, 0.1, 1, 10 100 nM) for 48 and 72 h or anti-PD-L1 (0, 0.1, 1, 10 100 μg/mL) for 48 h or with 10 nM EVE for different times (0, 24, 48, 72 h). As expected, EVE at 1 nM and above suppressed S6 phosphorylation and cell proliferation in a dose-dependent manner (Fig. 2a,b). After 72 h incubation with EVE, there was no recovery of mTOR activation or feedback activation of AKT. In contrast to EVE, anti-PD-L1 alone did not inhibit tumor cell proliferation (Fig. 2c), and in combination with 1 nM EVE (Fig. 2d) anti-PD-L1 did not enhance the effect of EVE.

EVE induces PD-L1 expression of tumor cells in an immunocompetent RENCA tumor-bearing mouse model. An *in vivo* study was conducted to evaluate the anti-tumor effect of EVE and determine the optimum dose for evaluating antitumor effects of co-administration of EVE and anit-PD-L1. We treated RENCA tumor-bearing mice with different doses of EVE (0.25–1.0 mg/kg per day) for 18 days. EVE inhibited tumor growth at doses of 0.25 mg/kg per day and above in a dose-dependent manner (Fig. S2). To investigate whether EVE induces PD-L1 upregulation in the tumor microenvironment, we treated RENCA tumors with vehicle or 0.25 mg/kg per day EVE for 7 days and removed tumor tissue to conduct IHC staining and flow cytometric analysis. Tumors from mice treated with EVE had an increase in PD-L1 expression compared with tumors from vehicle-treated mice (Fig. 3a). FCM analysis confirmed that PD-L1 expression was increased by EVE in tumor cells in the lymphocyte common antigen $CD45^{-}$ fraction (Fig. 3b,c). These studies indicate that mTOR inhibition is correlated with increased PD-L1 expression *in vivo*. Therefore, 0.25 mg/kg EVE was used in the co-administration study.

The combination of everolimus and anti-PD-L1 antibody decreases RENCA tumor growth. We next aimed to evaluate the efficacy of combining EVE and anti-PD-L1 using xenografted tumors in immunocompetent mice. Mice were assigned to one of four groups (control, EVE, anti-PD-L1, or a combination of EVE and anti-PD-L1) and treated for 14 days (Fig. 4a). Mice treated with a combination of EVE and anti-PD-L1 showed a significantly greater body weight, even in the presence of decreased tumor burden, than controls (Fig. 4b). Decreases in body weight were accompanied by the growth of the xenografted tumors in the control group (Fig. 4c), possibly due to tumor-related deleterious effects. The significantly higher final body weights in mice treated with a combination of EVE and anti-PD-L1 compared to the controls can be attributed to the inhibitory effects of the combined treatment on the growth of the RENCA tumors. Histological examinations revealed no

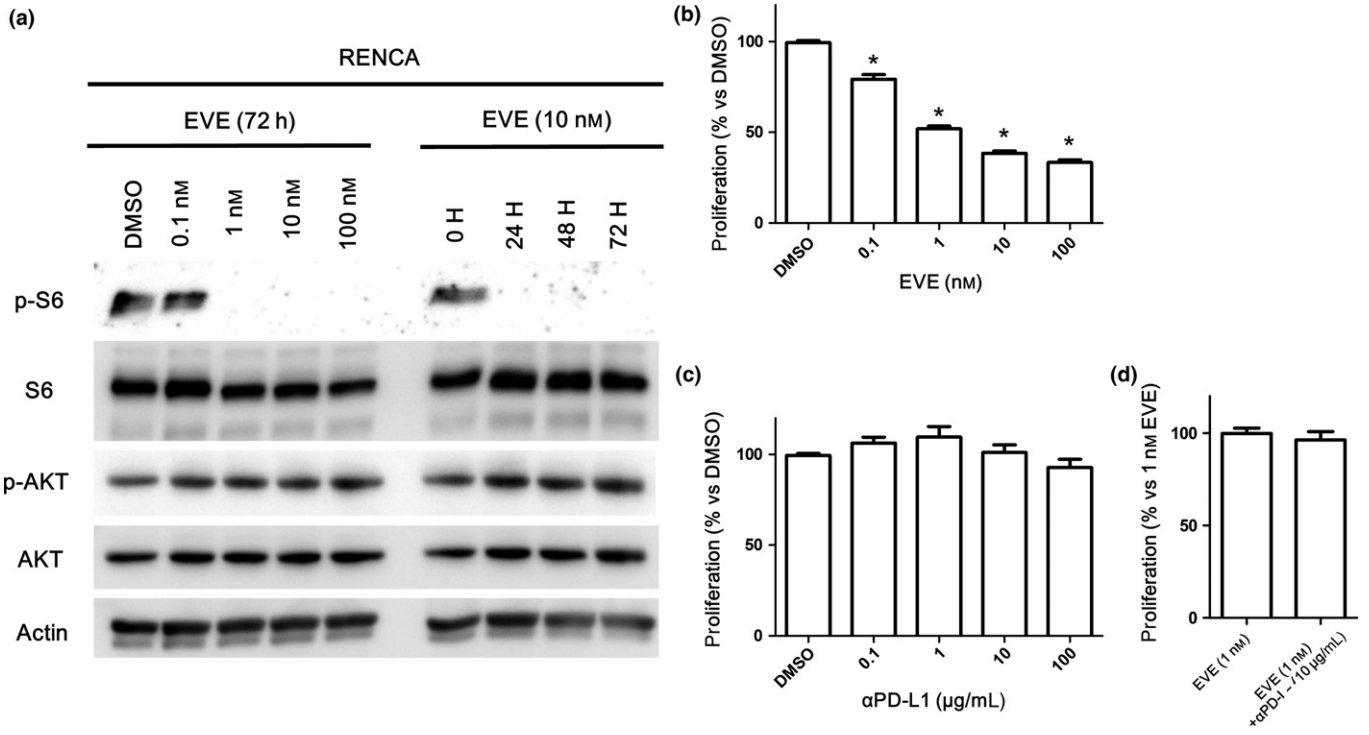

Fig. 2. Everolimus (EVE) inhibits the mTOR pathway and tumor cell proliferation *in vitro*. (a) Effect of EVE on the mTOR pathway in RENCA cells was determined by western blot analysis. Cells were treated with EVE (0, 0.1, 1.0, 10, 100 nM) for 72 h or EVE (10 nM) for 0–72 h. (b–d) RENCA cells were treated with EVE (0, 0.1, 1.0, 10, 100 nM), anti-PD-L1 (0, 0.1, 1.0, 10, 100 μg/mL), or the combination of EVE (1 nM) and anti-PD-L1 (10 μg/mL). After 48 h incubation, cell growth was evaluated by the WST-8 assay. *$P < 0.001$.

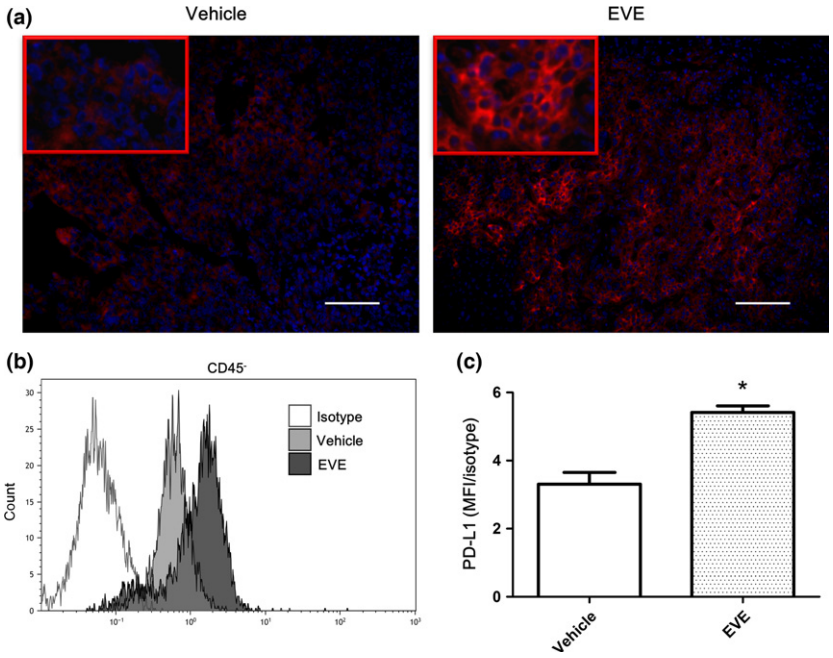

Fig. 3. Everolimus (EVE) induces programmed death-ligand 1 (PD-L1) expression in RENCA tumors *in vivo*. (a) IHC staining for PD-L1 in xenografted RENCA tumors treated with vehicle or 0.25 mg/kg per day EVE for 7 days (n = 3). (b) Representative histogram of PD-L1 expression in xenografted RENCA tumors. (c) PD-L1 expression by $CD45^-$ tumor cells in xenografted RENCA tumors was analyzed by flow cytometry (FCM). (n = 3) *P < 0.01. (Scale bar = 100 μM).

toxic alterations in the kidney, heart, liver, lung, or spleen in any of the groups (data not shown). EVE alone significantly decreased tumor burden compared to the control, whereas anti-PD-L1 alone did not. The combination of EVE and anti-PD-L1 significantly decreased tumor burden compared to EVE alone, anti-PD-L1 alone, and the control group (Fig. 4d,e).

Immunohistochemical analysis of pS6 (Fig. 5a) and p4EBP1 (Fig. S3a) revealed that EVE and combination therapy reduced mTOR activation in the tumor xenograft, while anti-PD-L1 had no effect on the expression level of pS6 and p4EBP1. To elucidate the mechanism of tumor suppression, we examined levels of proliferation and apoptosis. The Ki67 index was significantly decreased in the tumors from both the EVE and the combination of EVE and anti-PD-L1 treatment groups compared to the control, but there was no significant difference between tumors from the EVE alone and the combination of EVE and anti-PD-L1 treatment groups (Fig. 5b). However, tumors in mice treated with a combination of EVE and anti-PD-L1 showed an increase in apoptosis index compared to tumors from both the control and EVE alone treatment groups in the TUNEL analysis. There was a tendency for the apoptosis index to increase in the tumors of the anti-PD-L1 alone treated mice compared to the controls, albeit without statistical significance (Fig. 5c). Cleaved caspase-3 was also significantly increased in tumors in mice treated with the combination of EVE and anti-PD-L1 compared to the tumors in the control mice (Fig. S3b,c).

Next, to investigate the effect of EVE treatment alone and in combination with anti-PD-L1 on tumor infiltrating lymphocytes (TILs) that could contribute to the observed reduction in RENCA tumor growth, tumor tissue was examined for CD3, CD8, Granzyme B, and Foxp3 by immunohistochemistry. Tumors from mice treated with anti-PD-L1 had an apparent increase in the number of $CD3^+$ TILs and the ratio of cytotoxic $CD8^+$ T cells to TILs compared to the control, whereas tumors from mice treated with EVE alone did not. In contrast, combination therapy increased tumor infiltrating $CD3^+$ and the ratio of cytotoxic $CD8^+$ T cells to TILs compared to tumors from both the control and EVE alone treatment groups (Fig. 5d). Analysis of Granzyme B (a marker of T cell cytotoxicity) and Foxp3 (a marker of regulatory T cells (Tregs)) showed that the number of Granzyme B^+ cells and $Foxp3^+$ cells were significantly increased in tumors from the combination treatment group but not in the EVE or anti-PD-L1 alone groups compared to tumors from the control group (Fig. S4a, b). These results suggest that anti-PD-L1 enhanced the antitumor efficacy of EVE through induction of apoptosis and tumor infiltrating cytotoxic $CD8^+$ T cells.

Discussion

Malignant tumors possess mechanisms for evading host immune responses. Although multiple mechanisms contribute to immune system equilibrium, PD-L1 plays a prominent role in the tumor microenvironment.[21] PD-L1 is expressed in multiple types of malignancies and is associated with a high malignant grade of tumors, poor prognosis, and resistance to anti-cancer therapy.[15–17]

Everolimus is an oral mTOR inhibitor, recommended for RCC patients with previously failed anti-VEGF therapy. mTOR inhibition acts not only as an inhibitor of cell proliferation but also as an immunosuppressive agent. The immunosuppressive properties of mTOR inhibition have been investigated, and expansion of Tregs[22, 23] and promotion of M2 macrophage polarization[24] have been reported. However, the effects of EVE on PD-L1 expression in RCC are unclear. To predict the efficacy of and to optimize anti-PD-1/PD-L1 therapy, alone or in combination with an mTOR inhibitor, it is important to understand the impact of mTOR inhibition on PD-L1 expression in RCC tumors.

Our experiments revealed that the mTOR inhibitor EVE upregulated PD-L1 expression in RCC cell lines and xenografted tumor tissues. PD-L1 expression by tumor cells can inhibit T cell activity through its interaction with the PD-1 receptor expressed by tumor-specific T cells.[25] These findings suggest that EVE-induced PD-L1 upregulation may contribute to tumor escape from immune surveillance and promote tumor development. Thus, we hypothesized that blockade of PD-L1

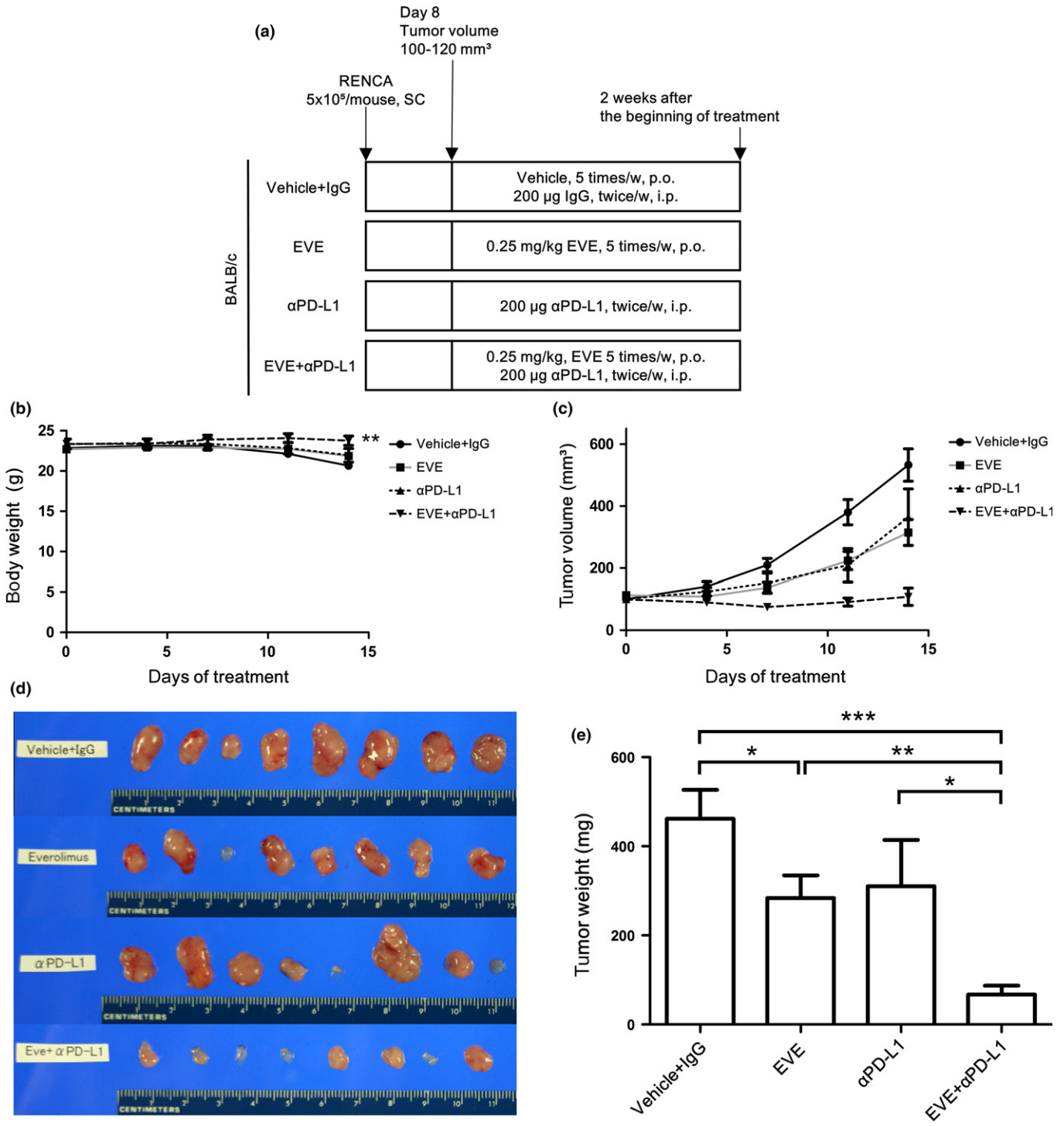

Fig. 4. The combination of everolimus (EVE) and anti-programmed death-ligand 1 (PD-L1) antibody suppresses RENCA tumor growth *in vivo*. (a) RENCA cells were injected subcutaneously into Balb/c mice. After tumors reached 100–120 mm^3, mice were treated with vehicle and IgG, EVE, anti-PD-L1, or a combination of EVE and anti-PD-L1 for 2 weeks. (n = 8) (b) Body weight changes over the duration of the experiment. (c) Xenograft tumor volumes. (d) Images of xenograft tumors at sacrifice. (e) Tumor weights at sacrifice. *P < 0.05; **P < 0.01; ***P < 0.001.

treatment could potentially enhance the anti-tumor effect of EVE, providing full cytotoxicity of host immunity against the tumor.

It has been reported that inhibition of the PD-1/PD-L1 axis reduces tumor growth independently of adaptive immunity in melanoma cells.[26] However, our study did not provide evidence of tumor growth suppression by anti-PD-L1 *in vitro*. Therefore, we combined EVE with anti-PD-L1 to treat murine RENCA RCC in an immunocompetent mouse model. The combination of EVE with anti-PD-L1 significantly reduced tumor burden compared with EVE alone. The impediment of tumor growth in those animals treated with the combination of

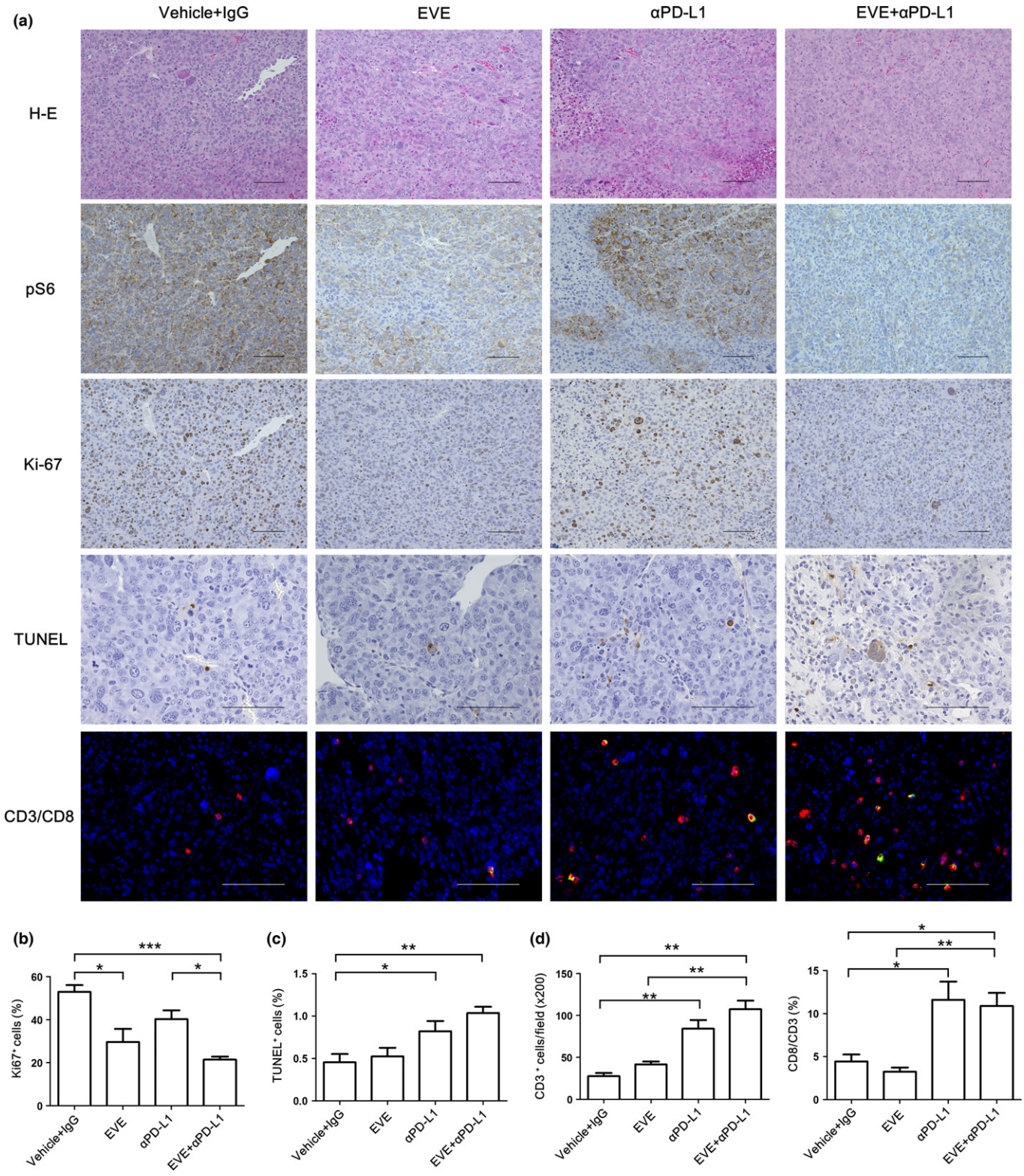

Fig. 5. (a) Images in the upper four rows represent Hematoxylin–Eosin and immunohistochemical staining (IHC) staining for pS6, Ki67, and terminal deoxynucleotidyl transferase-mediated dUTP nick end labeling (TUNEL) in tumors. Images in the bottom row represent IHC staining for CD3 (red), CD8 (green), and 4′6′-diamidino-2-phenylindole dihydrochloride (DAPI) (blue). Cytotoxic T lymphocytes are co-stained with CD3 and CD8. (b) Quantification of IHC staining for Ki67. (c) Quantification of TUNEL staining. (d) Quantification of IHC staining for $CD3^+$ cells and the ratio of $CD8^+$ to $CD3^+$ cells. Cells that were positive for Ki67, TUNEL, CD3 or CD8 staining were counted from three xenografts per treatment group. $^*P < 0.05$; $^{**}P < 0.01$; $^{***}P < 0.001$. (Scale bar = 100 μM).

EVE and anti-PD-L1 was also associated with an increase in the number of TILs and Granzyme B^+ cells in the tumors. Furthermore, combination therapy caused an increase of the ratio of cytotoxic $CD8^+$ T cells to TILs. Blockade of PD-L1 is a useful approach for improving antitumor immune responses, increasing the quality and quantity of tumor-specific $CD8^+$ T

cells.[27–29] Our results support the premise that tumor infiltrating cytotoxic $CD8^+$ T cells induce tumor apoptosis when anti-PD-L1 is combined with EVE. High expression of PD-L1 in the tumor appears to protect the tumor cells from $CD8^+$ T cells, leading to aggressive tumor invasion,[30] and the anti-PD-1 antibody nivolumab increased tumor infiltrating T cells, including $CD8^+$ T cells, in RCC patients.[31] These clinical discoveries support the relevance of the observations in our study to human tumors.

In human RCC, TILs themselves do not denote the efficacy of antitumor immunity, but tumor infiltrating $CD8^+$ T cells bearing proliferative activity could reflect effective antitumor immunity.[32,33] The cytotoxicity of $CD8^+$ T cells against the tumor is influenced by immunosuppressive factors in the local tumor microenvironment, such as cytokines released from innate immune cells, Tregs and myeloid derived suppressor cells, and signaling through immune checkpoint molecules including PD-1/PD-L1.[34,35] In the present study, EVE-induced PD-L1 upregulation within tumors suggest that EVE might prevent effective anti-tumor immunity. This provides a reasonable explanation for the enhanced antitumor effect of combined EVE and anti-PD-L1. Moreover, in our study model, blockade of PD-L1 alone was not sufficient to inhibit tumor growth despite inducing infiltration of $CD8^+$ T cells. Further clinical studies with pre- and on-treatment biopsy samples of RCC tumors are needed to investigate relationships between the tumor immune environment and the antitumor effect of EVE and anti-PD-L1.

In addition to our results, previous studies have demonstrated that chemotherapy and radiotherapy can also upregulate PD-L1 expression in tumor cells,[19,20,36,37] which may contribute to the acquisition of resistance to cancer therapy.[17] Our current findings indicate that blockade of the PD-1/PD-L1 axis may provide additional therapeutic benefits when combined with conventional anticancer therapy. In accordance with this reasoning, clinical trials combining anti-PD-L1 and current anti-angiogenic therapy are underway in patients with advanced renal cell carcinoma (NCT02231749, NCT01633970). However, there are no reported studies, either pre-clinical studies or clinical trials, examining the impact of the combination of an mTOR inhibitor with anti-PD-1/L1 therapy on RCC patients. Our study represents the first investigation into the impact of using an mTOR inhibitor in combination with anti-PD-L1 antibodies on tumor suppression using an immunocompetent mouse model of renal cell carcinoma.

The mechanism of PD-L1 expression is an area of active investigation. The regulation of PD-L1 is complex and depends not only on inflammatory cytokines but also on the status of underlying transcriptional and signaling networks that affect the cell cycle, proliferation, apoptosis, and survival.[18,38–42] Our study showed that blocking the mTOR pathway inhibits cell proliferation but increases expression of PD-L1. Further studies are needed to obtain a deeper insight into the molecular mechanisms underlying PD-L1 upregulation by EVE.

In summary, the present study demonstrated that while EVE increased PD-L1 expression in RCC cells *in vivo*, a combination of EVE with anti-PD-L1 treatment increased tumor infiltrating $CD8^+$ T cells and resulted in tumor regression. Additional preclinical data exploring the mechanism of the antitumor effects of EVE and anti-PD-L1 in RCC is therefore needed. Our study advances the current understanding of the role of PD-L1 in RCC, serving as a platform for developing new translatable immunotherapeutic options for the treatment of RCC.

Acknowledgements

This work was supported by Grant-in-Aid for Scientific Research from the Japan Society for the Promotion of Science (Grant No. 16K20157), and Smoking Research Foundation. The authors gratefully acknowledge the technical assistance of Rie Onodera, Keiko Sakata, Yuko Hisabayashi, and Yukiko Iura.

Disclosure Statement

The authors have no conflict of interest.

Abbreviations

EVE	everolimus
PD-1	programmed death-1
PD-L1	programmed death-ligand 1
RCC	renal cell carcinoma
TILs	tumor infiltrating lymphocytes

References

1 Ferlay J, Soerjomataram I, Dikshit R *et al.* Cancer incidence and mortality worldwide: sources, methods and major patterns in GLOBOCAN 2012. *Int J Cancer* 2015; **136**: E359–86.
2 Lipworth L, Tarone RE, Lund L, McLaughlin JK. Epidemiologic characteristics and risk factors for renal cell cancer. *Clin Epidemiol* 2009; **1**: 33–43.
3 Ljungberg B, Bensalah K, Canfield S *et al.* EAU guidelines on renal cell carcinoma: 2014 update. *Eur Urol* 2015; **67**: 913–24.
4 Escudier B, Porta C, Schmidinger M *et al.* Renal cell carcinoma: ESMO Clinical Practice Guidelines for diagnosis, treatment and follow-up. *Ann Oncol* 2014; **25**(Suppl. 3): iii49–56.
5 Motzer RJ, Escudier B, Oudard S *et al.* Efficacy of everolimus in advanced renal cell carcinoma: a double-blind, randomised, placebo-controlled phase III trial. *Lancet* 2008; **372**: 449–56.
6 Yang JC, Childs R. Immunotherapy for renal cell cancer. *J Clin Oncol* 2006; **24**: 5576–83.
7 Pardoll DM. The blockade of immune checkpoints in cancer immunotherapy. *Nat Rev Cancer* 2012; **12**: 252–64.
8 Weinstock M, McDermott D. Targeting PD-1/PD-L1 in the treatment of metastatic renal cell carcinoma. *Ther Adv Urol* 2015; **7**: 365–77.
9 Motzer RJ, Escudier B, McDermott DF *et al.* Nivolumab versus Everolimus in Advanced Renal-Cell Carcinoma. *N Engl J Med* 2015; **373**: 1803–13.
10 Chen DS, Irving BA, Hodi FS. Molecular pathways: next-generation immunotherapy–inhibiting programmed death-ligand 1 and programmed death-1. *Clin Cancer Res* 2012; **18**: 6580–7.
11 Butte MJ, Keir ME, Phamduy TB, Sharpe AH, Freeman GJ. Programmed death-1 ligand 1 interacts specifically with the B7-1 costimulatory molecule to inhibit T cell responses. *Immunity* 2007; **27**: 111–22.
12 Zou W, Chen L. Inhibitory B7-family molecules in the tumour microenvironment. *Nat Rev Immunol* 2008; **8**: 467–77.
13 McDermott DF, Drake CG, Sznol M *et al.* Survival, durable response, and long-term safety in patients with previously treated advanced renal cell carcinoma receiving nivolumab. *J Clin Oncol* 2015; **33**: 2013–20.
14 McDermott DF, Sosman JA, Sznol M *et al.* Atezolizumab, an anti-programmed death-ligand 1 antibody, in metastatic renal cell carcinoma: long-term safety, clinical activity, and immune correlates from a phase IA study. *J Clin Oncol* 2016; **34**: 833–42.
15 Thompson RH, Kuntz SM, Leibovich BC *et al.* Tumor B7-H1 is associated with poor prognosis in renal cell carcinoma patients with long-term follow-up. *Cancer Res* 2006; **66**: 3381–5.
16 Hino R, Kabashima K, Kato Y *et al.* Tumor cell expression of programmed cell death-1 ligand 1 is a prognostic factor for malignant melanoma. *Cancer* 2010; **116**: 1757–66.
17 Liu XD, Hoang A, Zhou L *et al.* Resistance to antiangiogenic therapy is associated with an immunosuppressive tumor microenvironment in metastatic renal cell carcinoma. *Cancer Immunol Res* 2015; **3**: 1017–29.

18 Ritprajak P, Azuma M. Intrinsic and extrinsic control of expression of the immunoregulatory molecule PD-L1 in epithelial cells and squamous cell carcinoma. *Oral Oncol* 2015; **51**: 221–8.
19 Wu CT, Chen WC, Chang YH, Lin WY, Chen MF. The role of PD-L1 in the radiation response and clinical outcome for bladder cancer. *Sci Rep* 2016; **6**: 19740.
20 Choueiri TK, Figueroa DJ, Fay AP *et al.* Correlation of PD-L1 tumor expression and treatment outcomes in patients with renal cell carcinoma receiving sunitinib or pazopanib: results from COMPARZ, a randomized controlled trial. *Clin Cancer Res* 2015; **21**: 1071–7.
21 Dong H, Strome SE, Salomao DR *et al.* Tumor-associated B7-H1 promotes T-cell apoptosis: a potential mechanism of immune evasion. *Nat Med* 2002; **8**: 793–800.
22 Battaglia M, Stabilini A, Migliavacca B, Horejs-Hoeck J, Kaupper T, Roncarolo MG. Rapamycin promotes expansion of functional $CD4^+$ $CD25^+$ $FOXP3^+$ regulatory T cells of both healthy subjects and type 1 diabetic patients. *J Immunol* 2006; **177**: 8338–47.
23 Strauss L, Czystowska M, Szajnik M, Mandapathil M, Whiteside TL. Differential responses of human regulatory T cells (Treg) and effector T cells to rapamycin. *PLoS ONE* 2009; **4**: e5994.
24 Han R, Gao J, Zhai H, Xiao J, Ding Y, Hao J. RAD001 (everolimus) attenuates experimental autoimmune neuritis by inhibiting the mTOR pathway, elevating Akt activity and polarizing M2 macrophages. *Exp Neurol* 2016; **280**: 106–14.
25 Abiko K, Mandai M, Hamanishi J *et al.* PD-L1 on tumor cells is induced in ascites and promotes peritoneal dissemination of ovarian cancer through CTL dysfunction. *Clin Cancer Res* 2013; **19**: 1363–74.
26 Kleffel S, Posch C, Barthel SR *et al.* Melanoma cell-intrinsic PD-1 receptor functions promote tumor growth. *Cell* 2015; **162**: 1242–56.
27 Hirano F, Kaneko K, Tamura H *et al.* Blockade of B7-H1 and PD-1 by monoclonal antibodies potentiates cancer therapeutic immunity. *Cancer Res* 2005; **65**: 1089–96.
28 Tumeh PC, Harview CL, Yearley JH *et al.* PD-1 blockade induces responses by inhibiting adaptive immune resistance. *Nature* 2014; **515**: 568–71.
29 Blackburn SD, Shin H, Freeman GJ, Wherry EJ. Selective expansion of a subset of exhausted CD8 T cells by alphaPD-L1 blockade. *Proc Natl Acad Sci USA* 2008; **105**: 15016–21.
30 Shi F, Shi M, Zeng Z *et al.* PD-1 and PD-L1 upregulation promotes CD8(+) T-cell apoptosis and postoperative recurrence in hepatocellular carcinoma patients. *Int J Cancer* 2011; **128**: 887–96.
31 Choueiri TK, Fishman M, Escudier B *et al.* Immunomodulatory activity of nivolumab in metastatic renal cell carcinoma. *Clin Cancer Res* 2016. doi: 10.1158/1078-0432.CCR-15-2839.
32 Nakano O, Sato M, Naito Y *et al.* Proliferative activity of intratumoral CD8 (+) T-lymphocytes as a prognostic factor in human renal cell carcinoma: clinicopathologic demonstration of antitumor immunity. *Cancer Res* 2001; **61**: 5132–6.
33 Bromwich EJ, McArdle PA, Canna K *et al.* The relationship between T-lymphocyte infiltration, stage, tumour grade and survival in patients undergoing curative surgery for renal cell cancer. *Br J Cancer* 2003; **89**: 1906–8.
34 Harter PN, Bernatz S, Scholz A *et al.* Distribution and prognostic relevance of tumor-infiltrating lymphocytes (TILs) and PD-1/PD-L1 immune checkpoints in human brain metastases. *Oncotarget* 2015; **6**: 40836–49.
35 Fridman WH, Pages F, Sautes-Fridman C, Galon J. The immune contexture in human tumours: impact on clinical outcome. *Nat Rev Cancer* 2012; **12**: 298–306.
36 Zhang P, Su DM, Liang M, Fu J. Chemopreventive agents induce programmed death-1-ligand 1 (PD-L1) surface expression in breast cancer cells and promote PD-L1-mediated T cell apoptosis. *Mol Immunol* 2008; **45**: 1470–6.
37 Qin X, Liu C, Zhou Y, Wang G. Cisplatin induces programmed death-1-ligand 1(PD-L1) over-expression in hepatoma H22 cells via Erk /MAPK signaling pathway. *Cell Mol Biol* 2010; **56**(Suppl): Ol1366–72.
38 Parsa AT, Waldron JS, Panner A *et al.* Loss of tumor suppressor PTEN function increases B7-H1 expression and immunoresistance in glioma. *Nat Med* 2007; **13**: 84–8.
39 Qian Y, Deng J, Geng L *et al.* TLR4 signaling induces B7-H1 expression through MAPK pathways in bladder cancer cells. *Cancer Invest* 2008; **26**: 816–21.
40 Ghebeh H, Tulbah A, Mohammed S *et al.* Expression of B7-H1 in breast cancer patients is strongly associated with high proliferative Ki-67-expressing tumor cells. *Int J Cancer* 2007; **121**: 751–8.
41 Zhu J, Chen L, Zou L *et al.* MiR-20b, -21, and -130b inhibit PTEN expression resulting in B7-H1 over-expression in advanced colorectal cancer. *Hum Immunol* 2014; **75**: 348–53.
42 Lee SJ, Jang BC, Lee SW *et al.* Interferon regulatory factor-1 is prerequisite to the constitutive expression and IFN-gamma-induced upregulation of B7-H1 (CD274). *FEBS Lett* 2006; **580**: 755–62.

Supporting Information

Additional Supporting Information may be found online in the supporting information tab for this article:

Fig. S1. After 786-O and RENCA cells were treated with EVE (0, 0.1, 1.0, 10, 100 nM), LY294002 (0, 0.1, 0.5, 2.5, 5.0 μM), or MK2206 (0, 0.1, 1.0, 10, 100 nM) for 72 h, PD-L1 expression was analyzed by FCM.

Fig. S2. (a) RENCA cells were injected subcutaneously into Balb/c mice. After tumors reached 100–120 mm^3, mice were treated with vehicle or EVE (0.25, 0.5, 1.0 mg/kg) for 18 days.

Fig. S3. (a) IHC staining for p4EBP1 in RENCA tumors. (b) IHC staining for cleaved caspase 3 in RENCA tumors. (c) Quantification of IHC staining for cleaved caspase 3.

Fig. S4. (a) Images represent IHC staining for Granzyme B and Foxp3 in RENCA tumors. (b) Quantification of IHC staining for Granzyme B^+ cells. (c) Quantification of IHC staining for $Foxp3^+$ cells.